JOURNAL OF MATERIALS SCIENCE **38** (2003) 533–540

The effect of low energy impact on the tensile strength of coated and uncoated glass particulate composites

G. C. PAPANICOLAOU*, S. P. GIANNIS
Composite Materials Group, Department of Mechanical and Aeronautical Engineering, University of Patras, Patras 265 00, Greece
E-mail: gpapan@meibm.mech.upatras.gr

K. IMIELINSKA
Department of Materials Science and Engineering, Technical University of Gdansk, Gdansk, Poland

The residual tensile strength of glass filled particulate composites has been determined after low energy impact for various energy values. The material systems constructed for the needs of this research consisted of epoxy resin filled with glass beads. The glass beads were either uncoated or alternatively coated with a reactive silane based bonding agent. Specimens with various filler volume fractions were available. The effect of silane coating as well as the filler volume fraction was analytically discussed. Finally, a model developed in previous work for continuous fibre reinforced composite laminates was adopted to describe the residual tensile strength after impact. In most of the cases the predicted curves fit the experimental results very well.

1. Introduction

Filled polymers are of great importance for modern technology. Incorporation of fillers in polymers allows regulation of mechanical and other properties of these materials. Filled polymers are very complicated heterogeneous systems, and it is difficult to describe theoretically their mechanical behavior. Thus, the effect of incorporating filler particles into a polymeric matrix on the physical and mechanical properties of the matrix material has been the subject of many investigations.

The incorporation of glass beads into some polymers leads to increase in the glass transition temperature (T_g), which appears to be strongly dependent on the filler volume fraction [1].

It is well known that due to their high stiffness, glass beads increase the modulus of a polymeric matrix material. Both treated and untreated glass particles give practically the same modulus values showing that interfacial properties are not important to the modulus. Different behavior is observed if tensile strength is examined for composites containing treated and untreated glass particles [2–6].

The effect of filler volume fraction and temperature on the energy absorbed by a sample of a particulate composite material tested in Charpy mode impact has also studied [7]. It was found that the impact energy absorbed reaches maximum values for temperatures above 120°C.

Finally, in order to improve the mechanical behaviour of laminated composites, many investigators [8, 9] have proposed the incorporation of small particles into the laminated composite material. Incorporation of polyethylene particles was found to improve the impact resistance of quasi-isotropic glass fibre reinforced polyester resin composites.

In the present paper the tensile strength after impact for specimens of various filler volume fractions was experimentally computed. A previously developed model for continuous fibre reinforced composites was adopted for the description of the residual tensile strength degradation after low energy impact. The new expression of the model takes into account the effect of the filler volume fraction as well as the treatment of the fillers.

2. Theoretical background

The theoretical model used in the present work is based on a previously developed model for continuous fibre reinforced composites [10]. In fact, it is the second attempt to extend the use of that model in order to predict the residual strength after impact of non-fibrous composite materials [11].

The model developed in reference [10] is based on the assumption that degradation of flexural stiffness matrix term, D_{xx}, is related to the residual strength after impact by:

$$\frac{\sigma_r}{\sigma_0} \cong \frac{D_{xx,r}}{D_{xx,0}} \tag{1}$$

where, σ_r represents the residual tensile strength of the impacted material, σ_0, is the strength of the unimpacted

*Author to whom all correspondence should be addressed.

material, $D_{xx,0}$ is the flexural stiffness matrix term of the unimpacted material corresponding to the longitudinal physical axis of the specimen and $D_{xx,r}$ is the respective flexural stiffness matrix term of the impacted material.

Through the analysis presented by Papanicolaou *et al*. [10] the final form of the model is given by the expression:

$$\frac{\sigma_r}{\sigma_0} = \frac{\frac{d}{U^\alpha}\sum_{\kappa=1}^{n}(\overline{M_\kappa})_0\left[Q_{xx,\kappa}\left(z_\kappa^3 - z_{\kappa-1}^3\right)\right]}{\sum_{\kappa=1}^{n}\left[Q_{xx,\kappa}\left(z_\kappa^3 - z_{\kappa-1}^3\right)\right]} = m\frac{d}{U^\alpha} \quad (2)$$

where, U is the impact energy, α is an energy absorption coefficient depended on the capacity of the material to absorb impact energy, d is a factor dependent on the material properties and test conditions and m is the ratio of summations dependent on material properties and stacking sequence of the laminate, defined as follows:

$$m = \frac{\sum_{\kappa=1}^{n}(\overline{M_\kappa})_0\left[Q_{xx,\kappa}\left(z_\kappa^3 - z_{\kappa-1}^3\right)\right]}{\sum_{\kappa=1}^{n}\left[Q_{xx,\kappa}\left(z_\kappa^3 - z_{\kappa-1}^3\right)\right]} \quad (3)$$

Here $(\overline{M_\kappa})_0$ is the mean value for the bending stiffness mismatching coefficient of the κ-lamina, $Q_{xx,\kappa}$ is the x-direction stiffness matrix term of the κ-lamina, z_κ is the distance of the κ-lamina from the middle plane of the laminate and n is the total number of plies in the laminate. The mean value of $(\overline{M_\kappa})_0$ is defined as follows:

$$(\overline{M_\kappa})_0 = \frac{(M_{\kappa-1,\kappa})_0 + (M_{\kappa,\kappa+1})_0}{2} \quad (4)$$

where, $(\overline{M_\kappa})_0$ refers to κ-lamina and $(M_{\kappa-1,\kappa})_0$ and $(M_{\kappa,\kappa+1})_0$ refer to the interfaces of the adjacent layers $(\kappa-1)$, κ and $(\kappa+1)$. The so-called bending stiffness mismatching coefficient $(M_{\kappa,\kappa+1})_0$ according to reference [12] express the difference in bending stiffness between two adjacent layers and it is defined as follows:

$$(M_{\kappa,\kappa+1})_0 = \frac{D_{xx,0}(\theta_\kappa) - D_{xx,0}(\theta_{\kappa+1})}{D_{xx,0}(0^\circ) - D_{xx,0}(90^\circ)} \quad (5)$$

Based on experimental results, a linear variation of α and d with the amount of the $\pm 45^\circ$ plies in the laminate was found [10].

The extension of the above model to particulate composites is based on the assumption that the behaviour of particulate composites is close to isotropic materials, so there is no property mismatch through the thickness of the material. Based on this assumption, the ratio of summations, m, can be estimated equal to 1. Equation 2 can be written alternatively as:

$$\mathrm{Log}\left(\frac{\sigma_r}{\sigma_0}\right) = -\alpha\,\mathrm{Log}(U) + \mathrm{Log}(d) \quad (6)$$

Using the experimental results for the fraction of tensile strength as a function of impact energy along with Equation 6, the coefficient α and constant $\mathrm{Log}(d)$ are estimated using least squares and they can also be related to the particle volume fraction, V_p, of the particulate composite material.

3. Materials and experiments

The materials were derived from diglycidyl ether of bisphenol A (EPIDIAN-6) epoxy system. Triethylene tetramine (TETA) was employed as the curing agent. Both epoxy resin and curing agent were produced by the chemical plants Organika–Sarzyna Co. Ltd. (Poland). The diluent for the resin was the dibuthyl ftalate. The rigid particulate fillers were glass beads with an average diameter of 60 μm supplied by the Interminglass Co. Ltd. (Poland).

The glass beads were either uncoated or alternatively coated with a reactive silane based bonding agent. This was a γ-glycidoxypropyltrimethoxysilane, which was applied by immersing the glass beads for 30 min in a 1% solution of ethanol water (95 : 5 by volume) then drying the glass beads for 1 h at room temperature, 4 h at 40°C and finally 1 h at 120°C.

Mechanical and physical properties for the inclusions as well as for the matrix material are shown in Table I while Table II presents the chemical composition of the particulate composite material.

For the preparation of the composite system the resin was first mixed with the diluent and heated in order for the entrapped air to be removed. Then the glass powder was added to the hot resin. The liquid material was thoroughly mixed, degassed in a vacuum chamber for 10 min, cooled to 40°C and then the curing agent was added. The liquid was again mixed and finally cast in to the preheated metal moulds. Powder was mixed with the diluted resin before adding the curing agent in order to allow better degassing of the mixture, improving the quality of adhesion of the phases. The plates were cured at room temperature for 48 h following post-curing at 100°C for 6 h.

The impact tests were conducted on a drop weight impact testing machine produced by the Department of Materials Science and Engineering, Technical University of Gdansk. Steel impactors with a hemispherical tup 12 mm in diameter were used. Three different

TABLE I Mechanical and physical properties of constituent materials

	Units	Glass beads	Epoxy resin
Young's modulus	GPa	71.00	3.60
Poisson's ratio	–	0.28	0.35
Density	Mgm^{-3}	2.50	1.20

TABLE II Chemical composition of glass epoxy particulate composites

Component	Composition (phr)
Epoxy resin: EPIDIAN – 6	100
Curing agent: TETA	12
Diluent: DIBUTHYL FTALATE	15
Reinforcement: GLASS PARTICLES	$0 < V_p < 50\%$

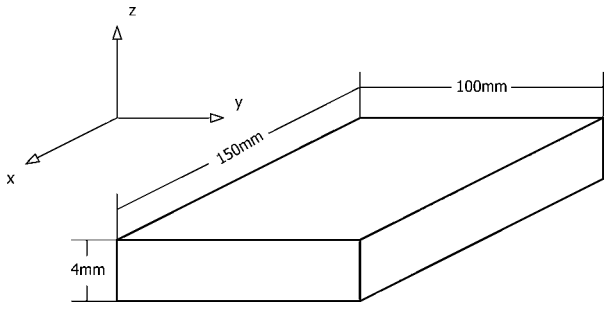

Figure 1 Plate in-plane dimensions for impact tests.

impactors were used 144, 122 and 115 g in weight. Varying the falling height of the impactor the impact energy varied from 2.5 J up to 8 J. Flat specimens having in-plane dimensions 150 × 100 × 4 mm have been manufactured using a diamond tooth rotating disk saw (Fig. 1). During impact tests the specimens were freely supported on a steel frame containing a hole 38 mm in diameter.

Finally, the impacted specimens were subjected to static tensile loading until ultimate failure, to determine their residual tensile strength. The tensile tests were conducted using Type I DIN 53 455 specimens with a crosshead speed up to 2 mm min^{-1}.

4. Results and discussion

Due to their high stiffness, glass beads increase the modulus of a polymeric matrix material as it is shown in Fig. 2 where the normalized composite modulus with respect to matrix modulus is plotted as a function of particle volume fraction. Both treated and untreated glass particles give practically the same modulus values showing that interfacial properties are not important to the modulus. On the other hand interfacial properties affect significantly the tensile strength of the particulate composite material leading to a decrease with increasing particle volume fraction, as expected [6]. The degradation is higher for the composites comprised of untreated glass beads (Fig. 3).

In Fig. 4 the experimental results of the residual tensile strength after low energy impact are plotted as a function of filler volume fraction, V_p, for the specimens with uncoated glass particles. As the filler volume fraction in the composite increases the residual tensile strength increases too. Same observations can be made examining Fig. 5, where the residual tensile strength for the specimens with silane coated glass particles is plotted versus V_p.

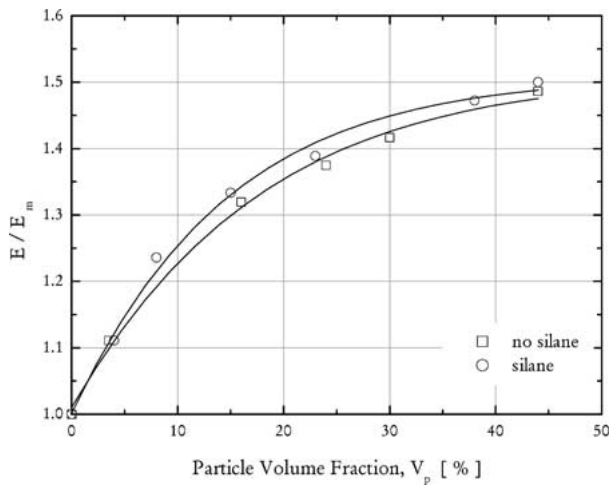

Figure 2 Variation of the normalized Young's modulus as a function of filler volume fraction for both silane coated and uncoated glass particles.

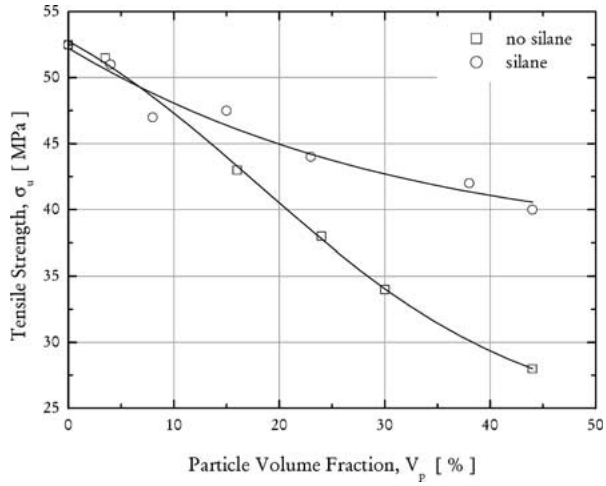

Figure 3 Variation of the initial tensile strength as a function of filler volume fraction for both silane coated and uncoated glass particles.

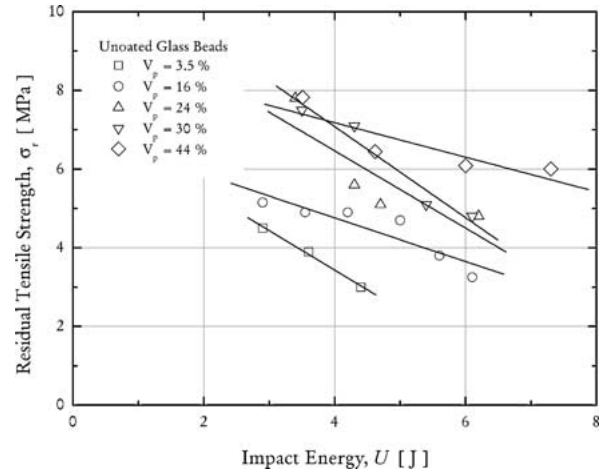

Figure 4 Variation of the residual tensile strength versus impact energy for various filler volume fractions—uncoated glass particles.

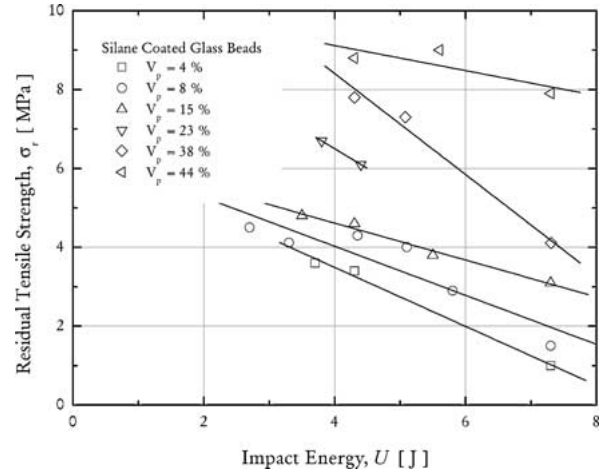

Figure 5 Variation of the residual tensile strength versus impact energy for various filler volume fractions—silane coated glass particles.

TABLE III Effect of silane coating on the residual strength values for a 44% particulate composite

Silane coated glass particles $V_p = 44\%$		Uncoated glass particle $V_p = 44\%$	
Impact energy (J)	Residual strength σ_r (MPa)	Impact energy (J)	Residual strength σ_r (MPa)
0	40.00	0	28.00
4.3	8.80	3.5	7.80
5.6	9.00	4.6	6.45
7.3	7.90	6.0	6.10
–	–	7.3	6.00

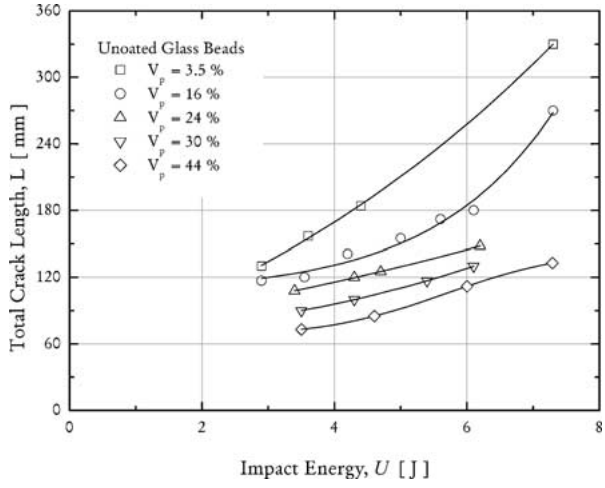

Figure 6 Variation of the total crack length versus impact energy for various filler volume fractions—uncoated glass particles.

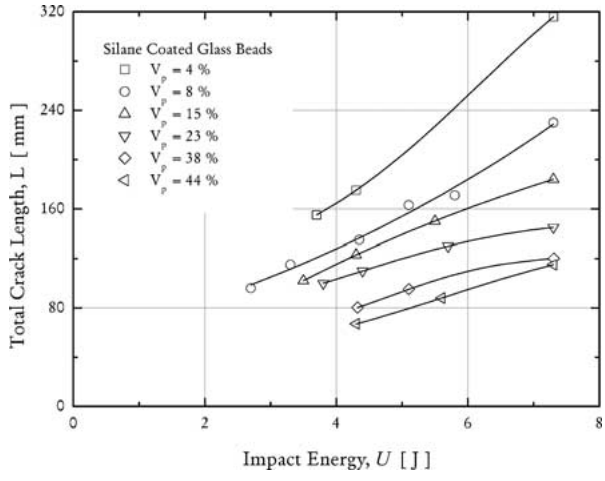

Figure 7 Variation of the total crack length versus impact energy for various filler volume fractions—silane coated glass particles.

Above remarks can be verified looking into the effect of filler volume fraction on the total crack length due to the impact loading. Increasing V_p, the total crack length decreases which indicates that the residual tensile strength will be higher for a particulate composite with high V_p than a composite with low V_p.

The same behaviour is observed for both coated and uncoated glass beads. The variation of the total crack length as a function of V_p is presented in Figs 6 and 7.

The effect of silane coating is clearly shown in Table III. For the same impact energy the residual tensile strength is higher for the material system containing

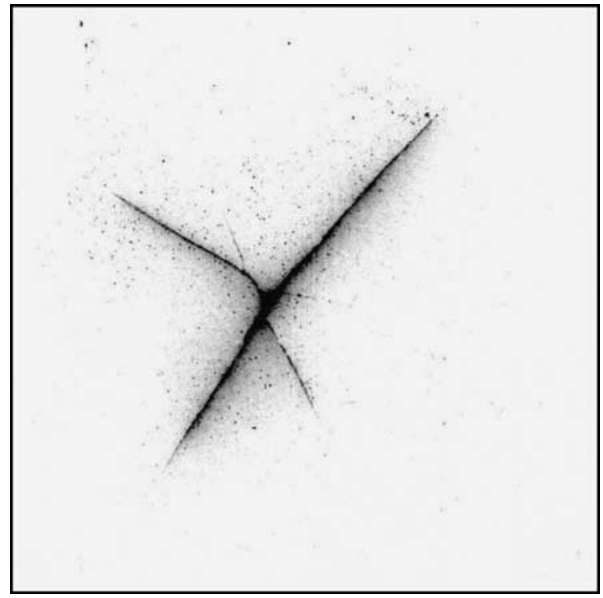

Figure 8 Photograph showing the crack due to 3 J impact on the surface of a specimen with filler volume fraction equal to 44%.

silane coated glass particles than the material system with the uncoated glass particles. More precisely, as it is shown in for an impacted specimen with 7.3 J particulate composite material ($V_p = 44\%$), the residual tensile strength after impact is equal to 6.45 MPa when there is no coating and 7.9 MPa when the particles are coated with silane.

Fig. 8 shows a typical crack on the surface of the composite plate. In particular it concerns a specimen with V_p equal to 44%, impacted in the middle with 3 J. It was noticed that the results of the tensile strength after impact were strongly dependent on the orientation of the cracks. If the longest crack happened to be oriented parallel to the tensile force direction and the cracks close to normal were very short the residual strength became higher.

In order to examine the crack path on the surface of impacted specimens, sections were obtained for both glass-silane/epoxy and glass/epoxy composites. The bottom surface of impacted specimens was ground and polished and then examined in a Tesla Scanning Electron Microscope at varying magnifications.

In glass-silane/epoxy systems most of the particles appear to be intact and adherent well to the matrix in contrast to the uncoated glass composites, where some of the glass particles seem to have fallen out of the sections indicating that interfacial debonding occurred during impact and crack propagation.

Both the coated and uncoated glass particles embedded in epoxy matrix result to impact energy dissipation through crack deflection arresting as well as particle debonding.

For the composite materials with silane coated glass particles the crack is shown to be traverse to the matrix region with deflections when the crack tip meets the particle. The glass particle fractured from the impact does not crumble out due to strong bonding with the resin (Fig. 9a). Also, it is observed that in the vicinity of the silane coated glass particles the crack does not follow the interphase between matrix and

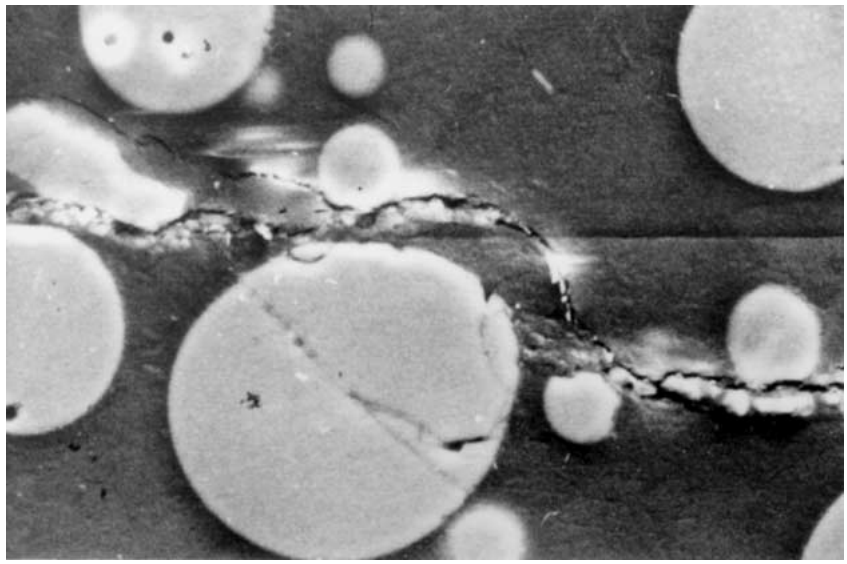

(a)

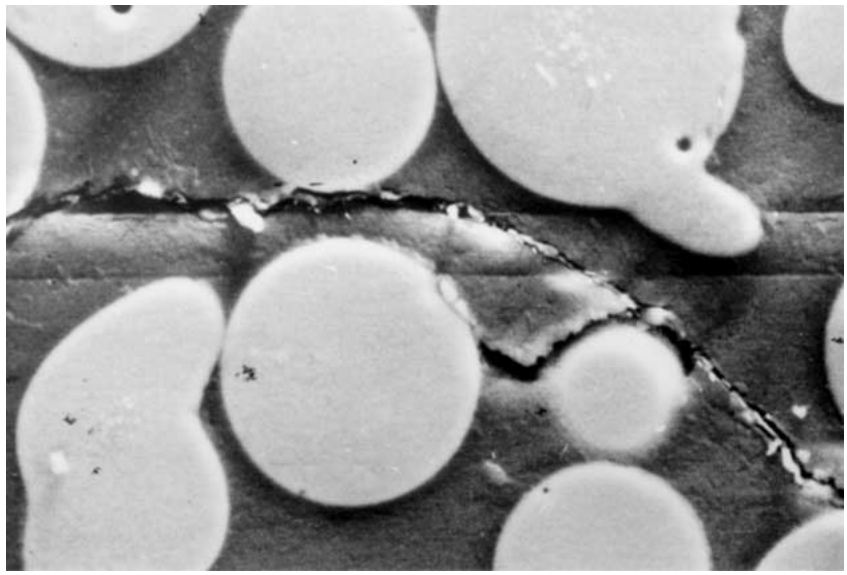

(b)

Figure 9 (a) Impacted area of a specimen containing silane coated glass particles (Scanning Electron Microscope ×600), (b) Impacted area of a specimen containing silane coated glass particles (Scanning Electron Microscope ×600).

filler, although it approaches the particle in this region (Fig. 9b).

For the composites with uncoated glass particles the crack propagation due to impact clearly follows the matrix—particle interphase, causing local debonding, which results in the particle crumble out (Fig. 10a and b).

In the present work in order to compare the theoretical predictions of the residual tensile strength derived by the model with the respective experimental findings the α-values as well as d-values for the application of the model are needed. Using Equation 6 along with the experimental results the unknown parameters can be estimated using least squares. Fig. 11 shows an example of the above procedure for a silane coated composite with V_p equal to 15%.

Repeating the last procedure for all available experimental data a linear variation of α and d with particle volume fraction was observed. In consequence two nomograms can be derived. The first one represents the variation of the energy absorption capacity factor α and coefficient d, with the filler volume fraction for silane coated glass particles while the second one represents the variation of the above parameters with the filler volume fraction for uncoated glass particles. These nomograms are shown in Figs 12 and 13, respectively. According to these nomograms the following relationships were derived for the particulate composites tested for silane coated and uncoated glass particles, respectively.

$$\alpha = 1 - 18.5 \times 10^{-3}\, V_p$$
$$d = 0.27 + 10^{-3}\, V_p \qquad (7)$$

$$\alpha = 1 - 14.3 \times 10^{-3}\, V_p$$
$$d = 0.21 + 7.5 \times 10^{-3}\, V_p \qquad (8)$$

Using Equations 7 and 8 the residual tensile strength after impact can be estimated for each V_p either for particulate composites with silane coated or alternatively uncoated glass particles.

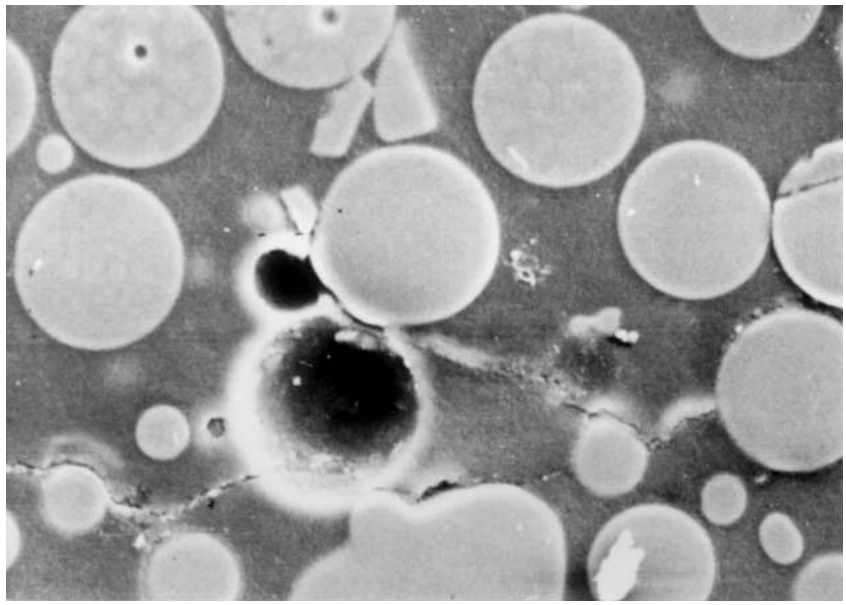

(a)

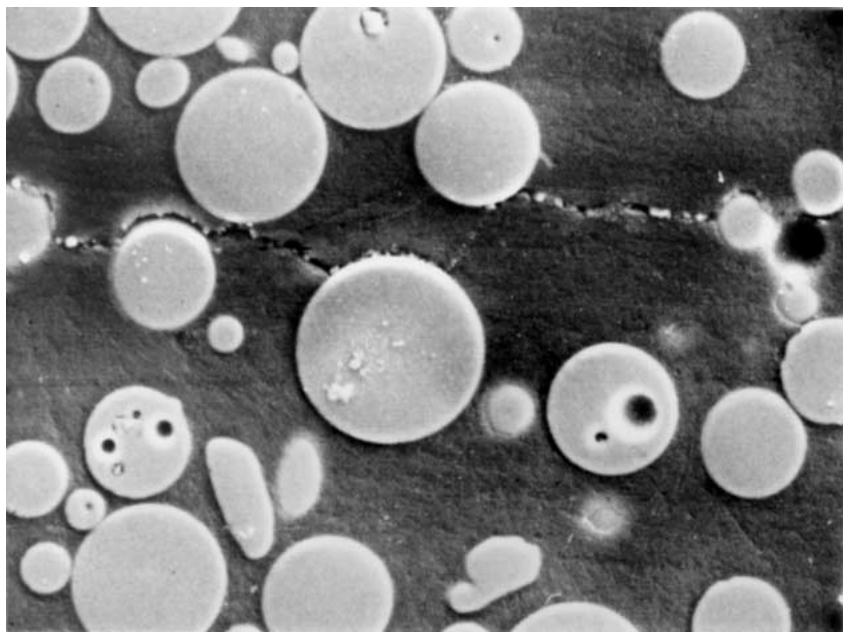

(b)

Figure 10 (a) Impacted area of a specimen containing uncoated glass particles (Scanning Electron Microscope ×600), (b) Impacted area of a specimen containing uncoated glass particles (Scanning Electron Microscope ×600).

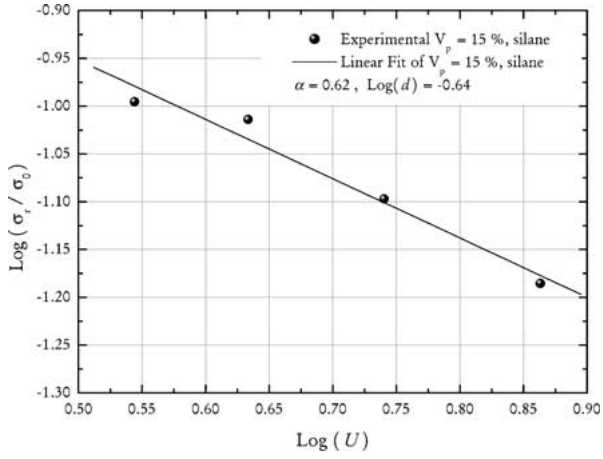

Figure 11 $\mathrm{Log}(\sigma_r/\sigma_0)$ vs. $\mathrm{Log}(U)$ plot for the determination of theoretical model parameters α and d.

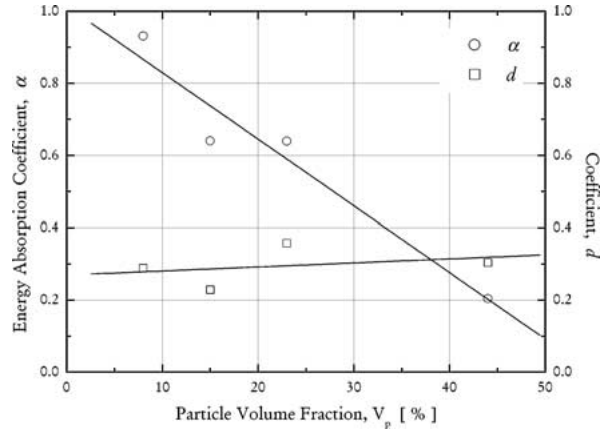

Figure 12 Nomogram of theoretical model parameters α and d versus V_P for silane coated glass particles.

TABLE IV Predicted and experimental values of the residual tensile strength for silane coated particles

Silane coated glass particles											
$V_p = 8\%$			$V_p = 15\%$			$V_p = 23\%$			$V_p = 44\%$		
U (J)	$(\sigma_r)_{\text{Exp}}$ (MPa)	$(\sigma_r)_{\text{Pr ed}}$ (MPa)	U (J)	$(\sigma_r)_{\text{Exp}}$ (MPa)	$(\sigma_r)_{\text{Pr ed}}$ (MPa)	U (J)	$(\sigma_r)_{\text{Exp}}$ (MPa)	$(\sigma_r)_{\text{Pr ed}}$ (MPa)	U (J)	$(\sigma_r)_{\text{Exp}}$ (MPa)	$(\sigma_r)_{\text{Pr ed}}$ (MPa)
2.70	4.50	5.61	3.50	4.80	5.48	3.80	6.70	5.99	4.30	9.68	10.53
3.30	4.12	4.72	4.30	4.60	4.72	4.40	6.10	5.50	5.60	9.90	10.03
4.35	4.30	3.73	5.50	3.80	3.95				7.30	8.69	9.55
5.10	4.00	3.26	7.30	3.10	3.22						
5.80	2.90	2.92									
7.30	1.50	2.40									

TABLE V Predicted and experimental values of the residual tensile strength for uncoated particles

Uncoated glass particles											
$V_p = 3.5\%$			$V_p = 16\%$			$V_p = 24\%$			$V_p = 44\%$		
U (J)	$(\sigma_r)_{\text{Exp}}$ (MPa)	$(\sigma_r)_{\text{Pr ed}}$ (MPa)	U (J)	$(\sigma_r)_{\text{Exp}}$ (MPa)	$(\sigma_r)_{\text{Pr ed}}$ (MPa)	U (J)	$(\sigma_r)_{\text{Exp}}$ (MPa)	$(\sigma_r)_{\text{Pr ed}}$ (MPa)	U (J)	$(\sigma_r)_{\text{Exp}}$ (MPa)	$(\sigma_r)_{\text{Pr ed}}$ (MPa)
2.90	4.50	4.43	2.90	5.15	6.24	3.40	7.80	6.39	3.50	7.80	9.50
3.60	3.90	3.60	3.55	4.90	5.34	4.30	5.60	5.46	4.60	6.45	8.59
4.40	3.00	2.98	4.20	4.90	4.69	4.70	5.10	5.14	6.00	6.10	7.78
			5.00	4.70	4.10	6.20	4.80	4.27	7.30	6.00	7.23
			5.60	3.80	3.76						
			6.10	3.25	3.52						

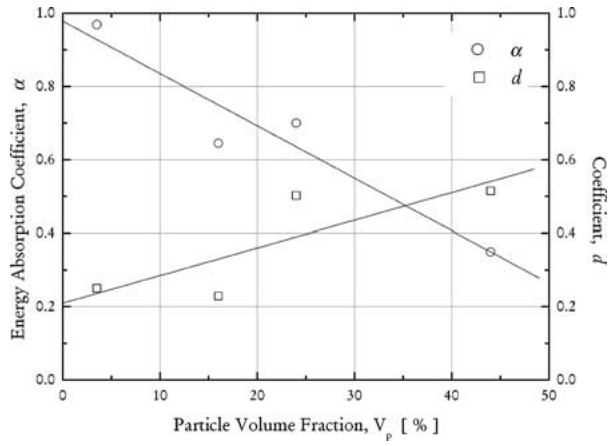

Figure 13 Nomogram of theoretical model parameters α and d versus V_P for uncoated glass particles.

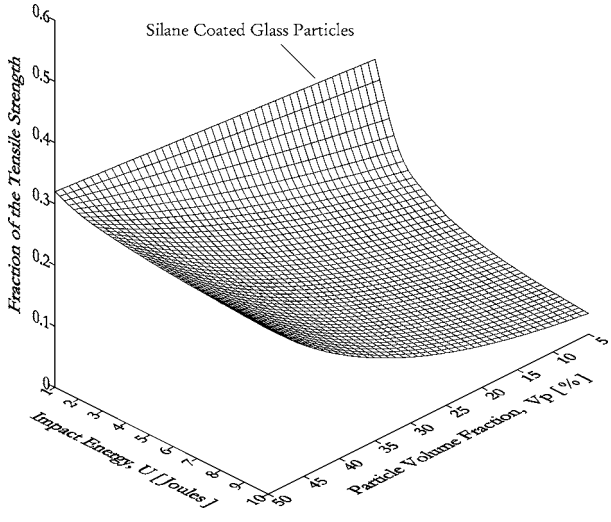

Figure 14 Surface plot of the fraction of the tensile strength for silane coated glass particles.

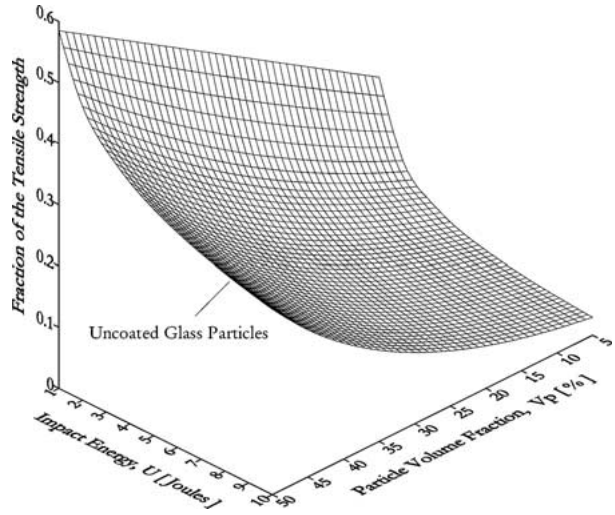

Figure 15 Surface plot of the fraction of the tensile strength for uncoated glass particles.

In Tables IV and V the predicted values of the residual tensile strength are listed along with the experimental results for coated and uncoated glass particles, respectively. As expected, the predicted curves fit the experimental findings very well.

Finally, based on Equations 7 and 8 a 3-dimensional representation of the variation of the fraction of the tensile strength with particle volume fraction and impact energy was made. In Fig. 14 the derived surface for the silane coated particulate composites is shown, while the respective surface for the uncoated particulate composite is presented in Fig. 15.

5. Conclusions

In the present work a model, previously developed by the authors to describe the strength degradation after

impact of continuous fibre reinforced composites, was extended in order to study the impact behavior of glass particulate composite materials. The model was used to generate useful nomograms for the investigation of the effect of low energy impact on the tensile strength of both coated and uncoated glass particulate composites. In addition, based on these nomograms, relationships between the model parameters α and d and the filler volume fraction, V_p, were derived.

The effect of silane coating on the residual tensile strength was also examined. For the same impact energy the residual tensile strength is higher for the material system containing silane coated glass particles than for the material system with the uncoated glass particles. Interfacial properties seem to be of great importance for the impact resistance of the particulate composites examined here.

References

1. T. K. KWEI and C. A.KUMINS, *J. Appl. Pol. Sci.* **8** (1964) 1483.
2. J. LEIDNER and R. T. WOODHAMS, *ibid.* **18** (1974) 1639.
3. M. R. PIGGOT and J. LEIDNER, *ibid.* **18** (1974) 1619.
4. L. NICOLAIS and R. V. MASHELKAR, *ibid.* **20** (1976) 561.
5. M. SCHRAGER, *ibid.* **22** (1978) 2379.
6. G. C. PAPANICOLAOU and D. BAKOS, *J. Rein. Plast. Compos.* **11** (1992) 104.
7. G. C. PAPANICOLAOU and A. G. ANDREOPOULOS, *Materials Chemistry and Physics* **18** (1987) 49.
8. V. K. SRIVASTANA and P. J. HOGG, *J. Mater. Sci.* **33** (1998) 1119.
9. G. PRITCHARD and Q. YANG, *ibid.* **29** (1994) 5047.
10. G. C. PAPANICOLAOU and C. D. STAVROPOULOS, *Composites* **26** (1995) 517.
11. G. C. PAPANICOLAOU, C. D. STAVROPOULOS, D. E. MOUZAKIS and J. KARGER-KOCSIS, *Plast. Rubber Compos., Process. Appl.* **26** (1997) 412.
12. D. LIU, *J. Compos. Mat.* **22** (1988) 674.

Received 14 December 2001
and accepted 4 September 2002